

# Experimental Study of the Radiative Decays $K^+ \rightarrow \mu^+ \nu e^+ e^-$ and $K^+ \rightarrow e^+ \nu e^+ e^-$

A. A. Poblaguev,<sup>4</sup> R. Appel,<sup>6,3</sup> G. S. Atoyan,<sup>4</sup> B. Bassalleck,<sup>2</sup> D. R. Bergman,<sup>6,\*</sup> N. Cheung,<sup>3</sup>  
 S. Dhawan,<sup>6</sup> H. Do,<sup>6</sup> J. Egger,<sup>5</sup> S. Eilerts,<sup>2,†</sup> W. Herold,<sup>5</sup> V. V. Issakov,<sup>4</sup> H. Kaspar,<sup>5</sup>  
 D. E. Kraus,<sup>3</sup> D. M. Lazarus,<sup>1</sup> P. Lichard,<sup>3</sup> J. Lowe,<sup>2</sup> J. Lozano,<sup>6,‡</sup> H. Ma,<sup>1</sup> W. Majid,<sup>6,§</sup>  
 S. Pislak,<sup>7,6,¶</sup> P. Rehak,<sup>1</sup> A. Sher,<sup>3</sup> J. A. Thompson,<sup>3</sup> P. Truöl,<sup>7,6</sup> and M. E. Zeller<sup>6</sup>

<sup>1</sup>Brookhaven National Laboratory, Upton, NY 11973, USA

<sup>2</sup>Department of Physics and Astronomy, University of New Mexico, Albuquerque, NM 87131, USA

<sup>3</sup>Department of Physics and Astronomy, University of Pittsburgh, Pittsburgh, PA 15260, USA

<sup>4</sup>Institute for Nuclear Research of Russian Academy of Sciences, Moscow 117 312, Russia

<sup>5</sup>Paul Scherrer Institut, CH-5232 Villigen, Switzerland

<sup>6</sup>Physics Department, Yale University, New Haven, CT 06511, USA

<sup>7</sup>Physik-Institut, Universität Zürich, CH-8057 Zürich, Switzerland

(Dated: April 5, 2002)

Experiment 865 at the Brookhaven AGS obtained 410  $K^+ \rightarrow e^+ \nu e^+ e^-$  and 2679  $K^+ \rightarrow \mu^+ \nu e^+ e^-$  events including 10% and 19% background. The branching ratios were measured to be  $(2.48 \pm 0.14(stat.) \pm 0.14(syst.)) \times 10^{-8}$  ( $m_{ee} > 150$  MeV) and  $(7.06 \pm 0.16 \pm 0.26) \times 10^{-8}$  ( $m_{ee} > 145$  MeV), respectively. Results for the decay form factors are presented.

PACS numbers: 13.20.Eb, 13.40.Ks

Chiral Perturbation Theory (ChPT) [1] has been a successful approach to describing the decays of pseudoscalar mesons. In the ChPT program radiative kaon decays can serve both as an important test and a source of input parameters for the theory. While the decay modes  $K^+ \rightarrow e^+ \nu \gamma$  ( $K_{e2\gamma}$ ) and  $\mu^+ \nu \gamma$  ( $K_{\mu2\gamma}$ ) have allowed some study of the form factors involved [2, 3, 4], the decays  $K^+ \rightarrow l^+ \nu e^+ e^-$  ( $K_{e2ee}$ ,  $K_{\mu2ee}$ ) allow a more detailed investigation into the structure of these decays. We report here on such an investigation from Experiment 865 at the Brookhaven National Laboratory AGS with a 100-fold increase in the number of events in the former mode and 150-fold increase in the latter [5].

The  $K_{e2ee}$  and  $K_{\mu2ee}$  decays are assumed to proceed via exchange of a  $W^+$ -boson ( $l^+ \nu$ ) and photon ( $e^+ e^-$ ). The decay amplitude [6, 7] includes inner bremsstrahlung (IB) corresponding to the tree diagrams in Fig. 1a,b, and structure dependent (SD) radiation (Fig. 1c) parameterized by vector  $F_V$ , axial  $F_A$  and  $R$  form factors.  $K_{e2\gamma}$  and  $K_{\mu2\gamma}$  experiments were actually sensitive only to  $|F_V + F_A|$ .  $R$ , which contributes only to decays with an  $e^+ e^-$ -pair, has not yet been measured.

Inner bremsstrahlung is unambiguously predicted by the  $K \rightarrow l \nu$  amplitude and is proportional to the kaon decay constant  $F_K = 160$  MeV. We included the kaon electromagnetic form factor in Fig. 1b (amplitude  $A_4$  of

Ref. [7]) in our definition of the IB term. The IB amplitude is negligible in  $K_{e2ee}$  decay due to electron helicity suppression, but dominates in  $K_{\mu2ee}$ . It contributes about 60% of the total  $K_{\mu2ee}$  branching ratio for invariant masses  $m_{ee} > 145$  MeV. An additional 20% comes from the IB and SD amplitude interference, which makes it possible to measure the signs of all form factors relative to  $F_K$ .

Generally form factors depend on  $W^2$  and  $q^2$ , where  $W$  and  $q$  are 4-momenta of the  $l^+ \nu$ -pair and of the photon ( $e^+ e^-$  pair), respectively. In our analysis we assume the dominance of low lying resonances [6]:

$$F_{V,A,R}^{(q^2, W^2)} = F_{V,A,R} / [(1 - q^2/m_\rho^2)(1 - W^2/\tilde{m}^2)] \quad (1)$$

where  $m_\rho = 770$  MeV, and  $\tilde{m} = m_{K^*} = 892$  MeV for  $F_V$  and  $\tilde{m} = m_{K_1} = 1270$  MeV for  $F_A$ ,  $R$ . Only the constants  $F_V$ ,  $F_A$ ,  $R$ , which we define in accordance with the Particle Data Group (PDG) [8], will be the subject of our analysis. The estimated uncertainties in the slope of form factors are taken as the model errors.

We also included in the analysis a hypothetical tensor amplitude

$$\frac{i e G_F V_{us}}{\sqrt{2}} F_T \epsilon^{\mu \nu \rho \sigma} \bar{u}_\nu (1 + \gamma^5) \sigma^{\mu \rho} v_l \quad (2)$$

since a possible tensor interaction has been discussed in regard to the  $\pi \rightarrow e \nu \gamma$  [9] and  $K \rightarrow e \nu \pi^0$  [10] experiments.

The experimental apparatus was constructed to search for the decay  $K^+ \rightarrow \pi^+ \mu^+ e^-$  in flight from an un-separated 6 GeV/c  $K^+$  beam, and has been described elsewhere [11]. The  $K_{e2ee}$  and  $K_{\mu2ee}$  data were obtained in a 1996 run simultaneously with that for a measurement of  $K^+ \rightarrow \pi^+ e^+ e^-$  ( $K_{\pi ee}$ ) [12]. The

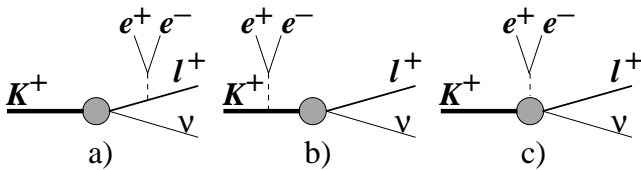


FIG. 1:  $K^+ \rightarrow l^+ \nu e^+ e^-$  decay diagrams

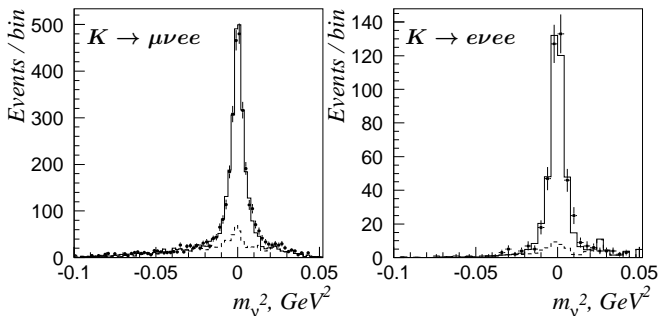


FIG. 2: Missing mass distributions for  $K_{\mu 2ee}$  and  $K_{e 2ee}$  decays. Error bars are data, dashed lines indicate background, and solid lines represent simulated distributions.

trigger for these modes allowed us to preselect events with three charged tracks, including an  $e^+e^-$  pair with high invariant mass  $m_{ee}$ . Prescaled decays  $K \rightarrow \pi\pi_D^0$  ( $K_{\pi 2}$ ),  $\mu\nu\pi_D^0$  ( $K_{\mu 3}$ ),  $e\nu\pi_D^0$  ( $K_{e 3}$ ),  $\pi\pi^0\pi_D^0$  ( $K_{\pi 3}$ ) followed by Dalitz decay  $\pi_D^0 \rightarrow e^+e^-\gamma$  with low  $m_{ee}$  were used for normalization.

Off-line the  $K_{e 2ee}$  and  $K_{\mu 2ee}$  candidates were required to have small missing neutrino mass,  $m_\nu$ . This missing mass was calculated using the measured decay product momenta and identities, and the centroid of the incident kaon beam momentum determined from  $K^+ \rightarrow \pi^+\pi^+\pi^-$  decays. After correction for the decay vertex dependence of the momentum, the kaon momentum resolution was  $\sigma_p/p = 1.3\%$  and the angular resolution  $\sigma_{\theta x} = \sigma_{\theta y} = 4$  mrad. The  $m_\nu^2$  distribution for each decay modes is displayed in Fig. 2. A cut  $|m_\nu^2| < 0.016$  GeV<sup>2</sup> isolated  $K_{l 2ee}$  decays.

Background in both cases was dominated by accidental overlap tracks. Events with one of the tracks out of time gave model independent samples of the accidental background. The samples were normalized by counting events with  $m_\nu^2 < -0.03$  GeV<sup>2</sup> with normalization uncertainties 8% for  $K_{\mu 2ee}$  and 25% for  $K_{e 2ee}$ . Other backgrounds and processes of interest were simulated using a GEANT3 [13] based Monte Carlo.

The  $K \rightarrow \pi ee$  decay is a potential background both for  $K_{e 2ee}$  and  $K_{\mu 2ee}$  decays. To suppress it, each event was tested as  $K_{\pi ee}$ . Events giving effective  $\pi ee$  mass and total momentum close to the beam kaon values were removed.

Cuts on the invariant  $e^+e^-$  mass  $> 145$  MeV ( $K_{\mu 2ee}$ ) and  $> 150$  MeV ( $K_{e 2ee}$ ) removed backgrounds associated with large branching ratio processes including a low mass  $e^+e^-$ -pair, *e.g.*  $K \rightarrow \pi\pi_D^0$ .

After the  $m_{ee} > 150$  MeV cut 410 detected  $K_{e 2ee}$  candidate events remain, including an estimated 35 accidental and 5  $K_{\pi ee}$  background events. The normalization sample was 86k  $K_{e 3}$  events and 2.3k  $K_{\pi 2}$  events. The accuracy of the normalization was estimated to be 4%, including the 1.5% error in the  $K_{e 3}$  branching ratio, a

1% trigger efficiency error, 2% for the radiative correction, and 3% for reconstruction efficiency. In evaluating the normalization factor we assumed that the  $\pi^0 \rightarrow ee\gamma$  branching ratio is 1.184%, from the QED calculation [14] with a form factor slope  $0.032 \pm 0.004$  [8].

The scintillation hodoscope embedded in the muon stack behind 40 cm of iron [11] was used for additional  $\mu/\pi$  separation in  $K_{\mu 2ee}$  analysis. The  $\mu/\pi$  detection efficiencies in the hodoscope were studied using  $K_{\pi 2}$  and  $K_{\mu 3}$  events where the  $\pi_D^0$  was fully reconstructed, *i.e.*, the resulting photon was observed and included in the kinematic reconstruction. The average efficiency of detecting muons with momentum greater than 0.9 GeV/c was 90%, while the probability of the misidentifying the pion as a muon was about 20%. Because GEANT simulation predicts a larger pion misidentification, the correction factor 0.85 was applied to the simulated efficiency of the pion detection. To reduce the uncertainty of this correction, the  $K_{\pi 2}$  decays in the normalization sample were additionally suppressed by a cut on  $E_\pi < 200$  MeV (calculated in the kaon center of mass). The final normalization sample contained 20.5k events including 16.2k  $K_{\mu 3}$ , 3k  $K_{\pi 3}$ , 0.8k  $K_{\pi 2}$ , and 0.4k accidentals. The normalization accuracy was estimated to be 5% including 2.5% from the  $K_{\mu 3}$  branching ratio, 1% from the trigger efficiency, 2% from radiative corrections, 3% from reconstruction efficiency and 2% from efficiency of  $\mu/\pi$  separation. The total number of the selected  $K_{\mu 2ee}$  events with  $m_{ee} > 145$  MeV was 2679, including an estimated background of 355 accidentals, 126  $K_{\pi ee}$ , and 33  $K \rightarrow \pi\pi_D^0\pi_D^0$  events.

In order to fit the data, we have used the logarithmic likelihood function

$$\mathcal{L} = \sum_i 2[m_i - n_i + m_i \ln(n_i/m_i)] - \frac{(N_{MC} - N_{MC}^{(0)})^2}{\sigma_{MC}^2} - \frac{(N_A - N_A^{(0)})^2}{\sigma_A^2} \quad (3)$$

Here,  $m_i$  and  $n_i$  ( $F_V, F_A, R, N_{MC}, N_A$ ) are the measured and calculated numbers of events in  $i$ -th bin of the 5-dimensional phase space (247  $K_{\mu 2ee}$  and 147  $K_{e 2ee}$  bins). We explicitly included the uncertainties,  $\sigma_{MC}$  and  $\sigma_A$ , in the Monte Carlo and accidental normalizations,  $N_{MC}$  and  $N_A$ , respectively in the fit.  $N_{MC}$  and  $N_A$  were regarded as independent parameters, while  $N_{MC}^{(0)}$  and  $N_A^{(0)}$  are the expected values from our studies discussed above.

The consistency between data and simulation was evaluated by significance level (SL) [8], *i.e.* the probability that a random repeat of the experiment would observe a smaller  $\mathcal{L}$ , assuming the model is correct. To calculate the SL we simulated the expected distribution of  $\mathcal{L}$ . In this calculation we explicitly accounted for possible variations of  $n_i$  due to the finite Monte Carlo and accidental statistics.

Fit results are summarized in Table I. In the combined

TABLE I: Fit to E865 data. The errors are  $\pm stat. \pm syst. \pm model$ . Results for the form factors  $F_V, F_A$ , and  $R$  (in units of  $10^{-3}$ ) are given for the fixed  $F_K = 160$  MeV and  $F_T = 0$ . Because the measurements of the form factors are correlated their linear combinations are also presented. Branching ratios BR (in units of  $10^{-10}$ ) were actually measured for  $m_{ee} > 145$  MeV ( $K_{\mu 2ee}$ ) and  $m_{ee} > 150$  MeV ( $K_{e2ee}$ ). All other values of BR are extrapolations.

	$K^+ \rightarrow \mu^+ \nu e^+ e^-$	$K^+ \rightarrow e^+ \nu e^+ e^-$	Combined Fit	Expected
$F_V$	124 ± 19 ± 13 ± 4	87 ± 30 ± 8 ± 5	112 ± 15 ± 10 ± 3	96 <sup>a</sup>
$F_A$	31 ± 21 ± 14 ± 5	38 ± 29 ± 11 ± 3	35 ± 14 ± 13 ± 3	41 ± 6 <sup>b</sup>
$R$	235 ± 25 ± 14 ± 12	227 ± 20 ± 10 ± 8	227 ± 13 ± 10 ± 9	230 ± 34 <sup>c</sup>
$F_V + F_A$	155 ± 25 ± 21 ± 5	125 ± 38 ± 12 ± 3	147 ± 21 ± 15 ± 4	± 144 ± 9  <sup>d</sup>
$F_V - F_A$	93 ± 32 ± 17 ± 7	50 ± 44 ± 15 ± 7	77 ± 20 ± 19 ± 6	102 ± 74 <sup>e</sup>
$R + F_V$	359 ± 36 ± 20 ± 14	314 ± 34 ± 11 ± 12	338 ± 19 ± 15 ± 11	
$R - F_V$	111 ± 26 ± 18 ± 11	139 ± 37 ± 12 ± 5	114 ± 20 ± 14 ± 8	
$R + F_A$	265 ± 9 ± 14 ± 7	265 ± 14 ± 10 ± 6	262 ± 6 ± 9 ± 6	
$R - F_A$	204 ± 46 ± 25 ± 17	189 ± 48 ± 18 ± 10	191 ± 27 ± 22 ± 12	
SL	11%	36%	12%	
$F_K$ (MeV)	157 ± 7 ± 5 ± 0.3	—	157 ± 5 ± 4 ± 0.2	160
$F_T$	-6 ± 13 ± 8 ± 1	$(32^2 \pm 37^2 \pm 25^2 \pm 6^2)^{1/2}$	-4 ± 7 ± 7 ± 0.4	0
$BR_{\text{total}}$	—	$(1730_{-540}^{+630} \pm 90 \pm 80)$ <sup>g</sup>	—	
$BR_{m_{ee} > 0.140}$	$(793 \pm 18 \pm 28 \pm 0.5)$ <sup>g</sup>	$(291 \pm 16 \pm 17 \pm 0.7)$ <sup>g</sup>	—	1300 ± 400 / $300_{-150}^{+300}$ <sup>f</sup>
$BR_{m_{ee} > 0.145}$	$706 \pm 16 \pm 26 \pm 0.4$	$(270 \pm 15 \pm 16 \pm 0.4)$ <sup>g</sup>	—	
$BR_{m_{ee} > 0.150}$	$(628 \pm 14 \pm 23 \pm 0.3)$ <sup>g</sup>	$248 \pm 14 \pm 14 \pm 0.2$	—	

<sup>a</sup> Theoretical value (axial anomaly)  $F_V/M_K = \sqrt{2}/8\pi^2 F$  [6, 7].

<sup>b</sup> ChPT to  $\mathcal{O}(p^4)$  extrapolation from  $\pi \rightarrow e\nu\gamma$  [7, 8].

<sup>c</sup>  $R/M_K = (1/3)F_K \langle r_K^2 \rangle$  [6], with the experimental value  $\langle r_K^2 \rangle = 0.34 \pm 0.05 \text{ fm}^2$  [15].

<sup>d</sup>  $K \rightarrow e\nu\gamma$  and  $K \rightarrow \mu\nu\gamma$  experimental data [2, 3, 4], corrected with the slopes (1) of the form factors [16].

<sup>e</sup>  $K \rightarrow \mu\nu\gamma$  experimental data [4].

<sup>f</sup> Previous  $K^+ \rightarrow \mu^+ \nu e^+ e^- / K^+ \rightarrow e^+ \nu e^+ e^-$  experimental data [5].

<sup>g</sup> Extrapolated value.

fit the likelihood function used was the sum of  $K_{\mu 2ee}$  and  $K_{e2ee}$  likelihood functions (3). Expectations for the measured values, included in Table I, are based on the previous  $K_{l2\gamma}$  and  $K_{l2ee}$  experiments, ChPT extrapolations of the  $\pi \rightarrow e\nu\gamma$  measurements, and theoretical predictions.

We considered three main contributions to the systematic error: (i) uncertainty of the detector efficiencies; (ii) uncertainty of the normalizations; (iii) errors due to the finite statistics of the accidental and Monte Carlo samples. All three contributions are comparable, and their quadratic sums are shown in Table I.

The model errors in Table I correspond to the uncorrelated sum of the 30% possible fluctuation of each slope of the form factors given in Eq. (1). Uncertainty in the  $dR/dq^2$  dominates the model errors of all form factors.

We include in Table I both measured and extrapolated branching ratios. The  $K_{\mu 2ee}$  total branching ratio is expected to be  $2.5 \times 10^{-5}$  [7]. Because of our cut of  $m_{ee} > 145$  MeV, and because  $K_{\mu 2ee}$  has a large probability of events at low  $m_{ee}$  due to its being dominated by IB, we are unable to determine the total branching ratio for that mode.

To evaluate the sensitivity of our data to the IB term, we have made a fit in which  $F_K$  in the definition of IB amplitude was regarded as a free parameter. The resulting value of  $F_K$  in Table I, being consistent with the expected value, also serves as a check of the normalization based on the  $K_{\mu 3}$  decay. The normalization based on the  $K_{e3}$  decay can not be checked in the same way in the  $K_{e2ee}$  analysis. However, we can alternatively determine that normalization by considering it as an unconstrained parameter in the combined fit. The ratio of this normalization to that obtained in  $K_{e3}$  was found to be  $(0.93 \pm 0.12)/(1.0 \pm 0.04)$ .

Using the current algebra relationship [6] between form factor  $R$  and kaon charge radius  $\langle r_K^2 \rangle$ ,  $R = (1/3)M_K F_K \langle r_K^2 \rangle$ , where  $M_K$  is the kaon mass, we can calculate  $\langle r_K^2 \rangle = 0.333 \pm 0.027 \text{ fm}^2$  in agreement with the direct measurement  $0.34 \pm 0.05 \text{ fm}^2$  [15]. The difference between our value and the experimental value of the pion charge radius  $\langle r_\pi^2 \rangle = 0.439 \pm 0.008 \text{ fm}^2$  [17] does not agree well with the ChPT prediction to  $\mathcal{O}(p^4)$ :  $\langle r_\pi^2 \rangle - \langle r_K^2 \rangle = (1/32\pi^2 F^2) \ln(M_K^2/m_\pi^2) = 0.036 \text{ fm}^2$  [7], where  $F = 92.4 \text{ MeV}$ .

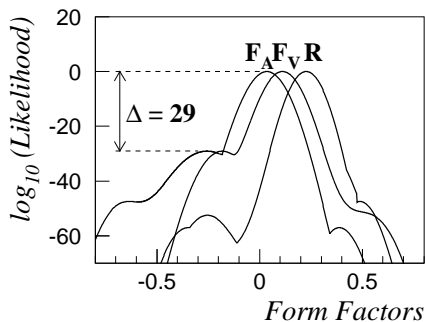


FIG. 3: Likelihood functions for form factors  $F_V$ ,  $F_A$ , and  $R$ .

If we assume that the form factors are constant instead of varying according to Eq. (1) we obtain for the mean values:  $F_V = 0.131$ ,  $F_A = 0.034$ ,  $R = 0.257$ . The value of  $\mathcal{L}$  indicates that constant form factors are less likely by a factor of 3.6 than those of Eq. (1).

While measurements of the  $K_{e2ee}$  decay can only determine the signs of the form factors relative to one another, due to the interference between the IB and SD amplitudes, knowledge of  $K_{\mu2ee}$  allows us to establish the signs relative to  $F_K$ . For the combined fit, the discrimination against wrong sign combinations is illustrated in Fig. 3.

The presentation of the tensor form factor for  $K_{e2ee}$  in Table I underlines that it is  $F_T^2$  which is measured in this mode. Our analysis of the  $K_{\mu2ee}$  decay is, however, sensitive to the sign of  $F_T$ . We did not find any evidence for the presence of a tensor term Eq. (2). Our result does not rule out the value  $F_T = -0.0056 \pm 0.0017$  [18] invoked as a possible interpretation [19] of the  $\pi \rightarrow e\nu\gamma$  data from Ref. [9]. Assuming that the  $K_{e3}$  tensor form factor is related to  $F_T$  as  $f_T/f_+ = 3.8F_T$  [20], we find  $f_T/f_+ = -0.02 \pm 0.04$  which strongly disagrees with value  $0.53^{+0.09}_{-0.10} \pm 0.10$  of Ref. [10]. A value compatible with 0 was also obtained in recent  $K_{l3}$  experiments [21].

To summarize, we have measured the  $K_{e2ee}$  and  $K_{\mu2ee}$  branching ratios:  $(2.48 \pm 0.14(stat.) \pm 0.14(syst.)) \times 10^{-8}$  ( $m_{ee} > 150$  MeV) and  $(7.06 \pm 0.16 \pm 0.26) \times 10^{-8}$  ( $m_{ee} > 145$  MeV), respectively. For the first time all  $K_{l2ee}$  form factors were unambiguously measured:  $F_V = 0.112 \pm 0.015 \pm 0.010 \pm 0.003(model)$ ,  $F_A = 0.035 \pm 0.014 \pm 0.013 \pm 0.003$ ,  $R = 0.227 \pm 0.013 \pm 0.010 \pm 0.009$ . Our analysis was especially sensitive to the sum of axial form factors  $R + F_A = 0.262 \pm 0.006 \pm 0.009 \pm 0.006$ . We did not find any inconsistency between  $K_{e2ee}$  and  $K_{\mu2ee}$  form factors. The measured inner bremsstrahlung contribution  $F_K = 157 \pm 5 \pm 4$  MeV agrees well with the theoretical expectation. No evidence of the tensor amplitude was found:  $F_T = -0.004 \pm 0.007 \pm 0.007$ . Our study of the form factors is more detailed but consistent with previous  $K(\pi) \rightarrow l\nu\gamma$  and  $K^+ \rightarrow l^+\nu e^+e^-$  experiments.

We thank J. Bijnens for his FORTRAN code describ-

ing the  $K^+ \rightarrow l^+\nu e^+e^-$  matrix element. We gratefully acknowledge the contributions to the success of this experiment by the staff and management of the AGS at the Brookhaven National Laboratory, and the technical staffs of the participating institutions. This work was supported in part by the U. S. Department of Energy, the National Science Foundations of the USA, Russia and Switzerland, and the Research Corporation.

\* Present address: Rutgers University, Piscataway, NJ 08855.

† Present address: The Prediction Co., Santa Fe, NM 87501.

‡ Present address: University of Connecticut, Storrs, CT 06269.

§ Present address: LIGO/Caltech, Pasadena, CA 91125.

¶ Present address: Phonak AG, CH-8712 Stäfa, Switzerland.

- [1] S. Weinberg, *Physica* **A96**, 327 (1979); J. Gasser and H. Leutwyler, *Ann. Phys.* **158**, 142 (1984); *Nucl. Phys.* **250**, 465 (1985).
- [2] K. Heard et al., *Phys. Lett.* **B55**, 324 (1975).
- [3] J. Heintze et al., *Nucl. Phys.* **B149**, 365 (1979).
- [4] S. Adler et al., *Phys. Rev. Lett.* **85**, 2256 (2000).
- [5] A.M. Diamant-Berger et al., *Phys. Lett.* **B62**, 485 (1976).
- [6] D. Bardin and E. Ivanov, *Sov. J. Part. Nucl.* **7**, 286 (1976).
- [7] J. Bijnens, G. Ecker, and J. Gasser, *Nucl. Phys.* **B396**, 81 (1993).
- [8] D. Groom et al., *Eur. Phys. J.* **C15**, 1 (2000).
- [9] V. Bolotov et al., *Phys. Lett.* **B243**, 308 (1990).
- [10] S. Akimenko et al., *Phys. Lett.* **B259**, 225 (1991).
- [11] R. Appel et al., *Nucl. Instrum. Methods Phys. Res., Sect. A* **479**, 349 (2002).
- [12] R. Appel et al., *Phys. Rev. Lett.* **83**, 4482 (1999).
- [13] GEANT Detector description and simulation tool, CERN Program Library, Long Writeup W5013 (1994).
- [14] B. E. Lautrup and J. Smith, *Phys. Rev.* **D3**, 1122 (1971).
- [15] S. Amendolia et al., *Phys. Lett.* **B178**, 435 (1986).
- [16] Our estimate based on the reanalysis of the published experimental data, gives the following corrections to the  $|F_V + F_A|$ :  $-0.012$  [2],  $-0.012$  [3],  $-0.008$  [4]. The last value may be compared with the authors' one  $-0.010$ , obtained in the real fit of the available data.
- [17] S. Amendolia et al., *Nucl. Phys.* **B277**, 168 (1986).
- [18] The tensor couplings in the pion and kaon decays are related here assuming the same Cabibbo angle for the tensor and V-A amplitudes [22].
- [19] A. A. Poblaguev, *Phys. Lett.* **B238**, 108 (1990).
- [20] We derived the factor 3.8 by comparing theoretical calculations of the tensor form factors in  $K_{l2ee}$  [22, 23] and  $K_{l3}$  [24]. We do not discuss the confidence of the cited calculations nor did we evaluate the accuracy of the factor 3.8.
- [21] S. Shimizu et al., *Phys. Lett.* **B495**, 33 (2000); A.S. Levchenko et al. (2001), hep-ex/0111048; I.V. Ajinenko et al. (2002), hep-ph/0202061.
- [22] E. Gabrielli, *Phys. Lett.* **B301**, 409 (1993).
- [23] V. Belyaev and I. Kogan, *Phys. Lett.* **B280**, 238 (1992).
- [24] M. Chizhov, *Mod. Phys. Lett.* **A8**, 2753 (1993).